

CONF 340142-8

NOTICE

PORTIONS OF THIS REPORT ARE AVAILABLE.

It has been reproduced from the best available copy to permit the broadest possible availability.

EFFECTS OF IMPROVED MODELING ON BEST ESTIMATE
BWR SEVERE ACCIDENT ANALYSIS*

C. R. Hyman and L. J. Ott
Oak Ridge National Laboratory

CONF-8410142--8

DE85 000593

To be presented at the
Twelfth Water Reactor Safety Meeting,
Gaithersburg, Maryland,
October 22-26, 1984.

By acceptance of this material, the publisher or recipient acknowledges the U.S. Government's right to retain a non-exclusive, royalty-free license in and to any copyright covering the article.

*Work done at Oak Ridge National Laboratory, operated by Martin Marietta Energy Systems, Inc. for U.S. Department of Energy under Contract No. DE-AC05-84OR21400.

DISCLAIMER

This report was prepared as an account of work sponsored by an agency of the United States Government. Neither the United States Government nor any agency thereof, nor any of their employees, makes any warranty, express or implied, or assumes any legal liability or responsibility for the accuracy, completeness, or usefulness of any information, apparatus, product, or process disclosed, or represents that its use would not infringe privately owned rights. Reference herein to any specific commercial product, process, or service by trade name, trademark, manufacturer, or otherwise does not necessarily constitute or imply its endorsement, recommendation, or favoring by the United States Government or any agency thereof. The views and opinions of authors expressed herein do not necessarily state or reflect those of the United States Government or any agency thereof.

MASTER

MP
DISTRIBUTION OF THIS DOCUMENT IS UNLIMITED

EFFECTS OF IMPROVED MODELING ON BEST ESTIMATE
BWR SEVERE ACCIDENT ANALYSIS*

C. R. Hyman
L. J. Ott

SASA Program

Oak Ridge National Laboratory

Introduction

Since 1981, ORNL has completed best estimate studies analyzing several dominant BWR accident scenarios.¹⁻⁴ These scenarios were identified by early Probabilistic Risk Assessment (PRA) studies and detailed ORNL analysis complements such studies. The results of ORNL efforts can be fed back into future PRAs to further refine their calculations. The base plant for all ORNL SASA work completed to date has been Unit One of the Browns Ferry Nuclear Plant, a BWR 4 with a Mark I containment.

In performing these studies, ORNL has used the MARCH code extensively.⁵ ORNL investigators have identified several deficiencies in early versions of MARCH with regard to BWR modeling.^{2,4} Some of these deficiencies appear to have been remedied by the most recent release of the code.⁶

Scope

It is the purpose of this paper to identify several of these deficiencies (some of which have not been remedied) and to examine the effect of improved modeling on calculated results.

To further refine the subject matter of this paper, all the information presented henceforth concerns the degraded core thermal/hydraulic analysis associated with each of the ORNL studies. This includes calculations of the containment response. The period of interest is from the time of permanent core uncover to the end of the transient. Specific objectives include the determination of the extent of core damage and timing of major events (i.e., onset of Zr/H₂O reaction, initial clad/fuel melting, loss of control blade structure, etc.). As mentioned previously the major analysis tool used thus far was derived from an early version of MARCH.⁵

*Research sponsored by the Office of Nuclear Regulatory Research, U.S. Nuclear Regulatory Commission under Interagency Agreement DOE 40-551-75 with the U.S. Department of Energy under contract DE-AC05-84OR21400 with the Martin Marietta Energy Systems, Inc.

Model Features

In work done by ORNL, it is clear that there are several features of BWRs which must be modeled. These features include channel boxes (canisters) and control blades, safety relief valve (SRV) cycling, vessel water level, and the large inventory of relatively cold water in the vessel which is not in direct contact with the core. The importance of modeling each of these BWR features will be discussed.

The BWR core houses many control blades and as can be seen in Fig. 1, each is surrounded by four fuel assemblies. Each fuel assembly consists of an array of fuel rods and water rods surrounded by a metal canister. The cladding material for the fuel rods is zirconium and the material making up the canister and the water rods is also zirconium. The neutron poison in the control blades is boron carbide powder (B_4C) housed inside hollow stainless steel rods. Water coolant is present both inside the canisters adjacent to the fuel rods and outside the canisters between the canisters and the control blade. The fluid inside the canisters receives a different heat input than the fluid in the interstitial region outside of the canisters. For the covered region this differing heat input affects the steaming rate both inside and outside the canisters. In the uncovered part of the core this different heat input results in different steam temperatures. Also the flow rates inside and outside the canister are different as flow inside the canister is controlled by an orifice located at the bottom of each fuel assembly. Therefore it is obvious that the thermal hydraulic environment that the incore structures are subjected to is not radially uniform.

It is also clear that lumping the UO_2 from the fuel rods with the zirconium from the canisters, fuel rods, and water rods is not desirable. This is because of several reasons. First is the fact that the thermal hydraulic environment of the fuel rods and canisters is different. Second, about 33% of core wide zirconium is located in the canisters where internal heating due to decay heat does not exist. Third, the artificial heat capacity of such a lumped mass is not typical of either the fuel rods or the canister.

As a result, ORNL has developed explicit models for the control blades and channel boxes analogous to the fuel rod models originally in MARCH.⁵ In fact, the BWR core models employed in MARCH 2.0 (ref. 6) are essentially the earliest version of the current ORNL models and were supplied to Battelle in January, 1983.

The next feature of BWRs which requires explicit modeling is the operation of the safety relief valves (SRVs). In BWRs, multiple SRVs protect the primary system from over-pressurization. Each has its own automatic opening and closing pressure setpoints with the closing pressure setpoint typically being 50 to 100 psi ($3.447 \cdot 10^5$ to $6.895 \cdot 10^5$ Pa) lower than the opening setpoint. These valves are large flow capacity devices and each can pass up to 6 1/2% of the full power steam flow. They can be operated manually. At low reactor vessel pressure, the flow

through the valves can become unchoked. The depressurization transients that each valve produces before closing causes the two-phase region to swell considerably. This increase in the level swell provides much better cooling to the previously uncovered regions of core and also provides considerable steam flow, an important parameter influencing the zirconium/steam reaction. As a result it is undesirable, in a best estimate sense, to model SRVs as devices which only limit the upper pressure at which the primary system can exist. The impact of the cyclical nature of SRV operation has a very dynamic impact on the thermal hydraulic behavior of the core.

The next feature which must be explicitly taken into account is the calculation of the collapsed liquid level inside the reactor vessel. As shown in Fig. 2, the reactor vessel is filled with various structures. These include the control rod guide tubes, jet pumps, upper plenum shell, core structures, the steam standpipes and separators, and the steam dryers. As can be imagined, the free volume inside the reactor vessel is not a simple function of height above vessel zero. Because level is an important controlling parameter under accident as well as normal operating conditions, ORNL has devoted considerable effort to determine the free volume as a function of height. Tables of free volume versus height for several regions internal to the reactor vessel have been constructed. These regions include (1) liquid inventory in the lower head and jet pumps, (2) liquid inventory in the region external to the core shroud, upper plenum, standpipes and separators but internal to the reactor vessel, (3) region inside the separators, standpipes, and the upper plenum, (4) region inside the canisters, (5) interstitial region outside the canisters, and (6) region normally occupied by steam but which under accident conditions may be occupied by water.

The reason for such a division of the reactor internal free volume is because of the different temperatures of water residing in these regions. Various ECC systems inject water at different temperatures into the reactor vessel at various locations. The control rod drive cooling water enters through the control rod guide tubes and therefore is injected into region 5. The high pressure injection systems, HPCI and RCIC, inject water into region 2. The low pressure injection system, LPCI injects through the recirculation pump return lines and thus injects through the mouth of the jet pump into region 1. The low pressure core spray injection system injects into regions 4 and 5. Each of these regions has its own temperature, and as a result each is modeled separately in the ORNL version of MARCH.

Mass and energy are conserved for each of these fluid volumes. Since no momentum equation is specified, the code at the present time calculates mass flows based on the very crude approximation of a vessel wide uniform collapsed liquid level. There is no spatial distribution of pressure. The solution algorithm proceeds as described in the following paragraph.

The essential idea is that each region has its own mass and as a result its own liquid volume at the beginning of each transient timestep. The code then updates the mass and enthalpy in each region due to water injection and for the case of regions 4 and 5 due to heat transfer from core structures to the water. At this point a steaming calculation is performed whereby the beginning of timestep pressure is assumed constant over the timestep and comparisons of updated region enthalpy with saturated liquid enthalpy determines the amount of steaming from each region. The total steaming rate is determined. Given the total steaming rate, the beginning of timestep gas inventory and temperature in the upper head, and coupled with a reduced timestep marching algorithm, the amount of gas leaving the system and the final system pressure can be determined. At this point the total mass and enthalpy (and thus volume) of the liquid is known and therefore a uniform collapsed liquid level can be determined. The code then calculates the amount of mass and enthalpy which must flow from one region to another so that the total mass and total enthalpy are conserved along with matching the requirement of uniform collapsed liquid level.

Inherent in the above calculational procedure is the requirement of being able to accurately calculate the total thermodynamic pressure of a mixture of steam and hydrogen given the temperature and volume as well as the mass of each species. The importance of such an accurate determination of system pressure should be clearly understood. It is the primary variable influencing the steaming calculation which in turn determines level swell, the importance of which has been discussed previously. As a result ORNL has adopted the Redlich-Kwong-Soave equation of state for mixtures of hydrogen and steam. It appears to be a satisfactory first order correction to the ideal gas law.

In addition to being able to accurately determine the pressure of a mixture of hydrogen and steam, additional thermophysical properties of a mixture of the two gases are required for evaluation of heat transfer correlations. ORNL uses either mass fraction or mole fraction weighted properties of each of the pure substances to obtain mixture properties. As a result ORNL has included a comprehensive physical properties package for hydrogen and water.

The final model that we have incorporated into our version of MARCH is a model which separates fuel and cladding in the fuel rods. The reason for this was the possibly non-conservative calculation of cladding temperature which is the sole dynamic parameter influencing the exothermic zirconium-steam chemical reaction. Previous versions of MARCH did not allow for separation of fuel and cladding and therefore produced a lumped node temperature which may not accurately depict cladding temperatures.

Results

Results of a calculation where each of the previously described models have been used will now be presented and compared with results of a calculation performed with an earlier ORNL version of MARCH. We had intended to provide comparisons with the latest Battelle version of MARCH, i.e., MARCH 2.0 (V151).⁶ We were able to get the code to execute the BWR MARK III sample problem but were unable to get it to execute our problem, a loss of decay heat removal transient. The calculation appears to have been trapped in an infinite loop somewhere in the containment part of the calculation. We have notified Battelle and have sent them copies of our input and output. However, because this difficulty has not been resolved we are unable to provide comparisons of our code's results from those generated from MARCH 2.0 (ref. 6).

Table 1 lists model differences between the old ORNL MARCH version and the current ORNL MARCH version. As the table shows, the only model upgrades which were present in the old version were the BWR canister and control blade models (includes independent evaluation of meltdown models for both the control blade and the canisters), and a partially upgraded H₂/H₂O physical properties package. All other models in the old version were those which were extant in the original version of MARCH.⁵

ORNL believes that there are six model upgrades which are particularly relevant to the loss of decay heat removal calculation. These include: (1) the use of an improved heat transfer correlation in the uncovered region of the core, (2) mechanistic rod models in the water covered region, (3) the new algorithm for calculation of pressure and leak rates, (4) multi-node analysis of in-vessel water inventory, (5) new boiling and flashing algorithm, and (6) the new collapsed liquid level model.

Comparisons of calculated results between the old and new ORNL versions of MARCH show the integrated effects produced as a result of the new models. Figure 3 presents the calculated pressure results from the new version. It is obvious that the SRV models in the new version tightly control the pressure in the primary system to between ~1050 and ~1120 psia (7.24×10^6 to 7.72×10^6 Pa). The SRV model in the old MARCH version, Fig. 4, was not able to maintain as tight a band as the new version because the number of SRVs it could open was user specified and because of difficulties (non-realisms) in the flashing and pressure calculation algorithm. Therefore, if the depressurization resulting from opening the SRVs produced a steaming rate larger than the flow capacity of the SRVs, the pressure of the system rose above the SRV set-point. This over-pressurization is not realistic. In the new version, the more realistic vessel pressure response in Fig. 3 (only one SRV cycled during this transient) primarily results from the improved (1) boiling (and flashing), (2) pressure, and (3) SRV models. The number of SRV cycles shown in Fig. 3 (from start to core uncover at 2255 mins) has been confirmed by hand calculations.

Figures 5 and 6 show the calculated collapsed liquid level (CLL) from the new and old versions respectively. Because of the differences in modeling the invessel water inventory, we could not simultaneously match the CLL and the total liquid mass of the system at the beginning of the calculation. As a result, we chose to match the CLL which is the more important parameter from the reactor operator point of view.

Comparisons of Figs. 5 and 6 show that the old version produces a more rapid fall in the CLL than the new version. This is the result of the differences in rod models between the two versions for the covered region of the core. Because this comparison points out a fundamental deficiency of the old model, an explanation will be given.

In calculating the heat balance for the water, the old ORNL version of MARCH formulates a so called "quench"⁵ parameter. This parameter is basically a change in internal energy of the fuel rods below the swollen mixture level and is positive when the rod internal energy is decreasing. This term is added to the decay heat produced in the covered sections of the core to get the net energy delivered to the fluid. For cases where the internal energy of the rods are increasing, the old ORNL version of MARCH sets the "quench" term to zero but still adds the whole amount of decay heat below the swollen level to the fluid. No accounting for increasing rod internal energy changes are made. As a result, the old ORNL version of MARCH adds too much energy to the covered region during periods of the calculation where rod internal energy and thus temperatures are increasing.

This deficiency produces no error when the SRVs open and the primary system depressurizes. The reason for this is because the saturation temperature of the fluid can drop by as much as 8°F (4.44 K) thus also lowering the rod temperatures and producing the appropriate energy transfer to the fluid. However, after the SRV closes, the pressure begins to rise and the fuel temperature follows the rising saturation temperature. Because of the previously defined deficiency in the old ORNL version of MARCH, too much energy is deposited in the fluid and the boiloff is artificially enhanced.

In the new ORNL version of MARCH, proper accounting of the internal energy changes of the rods are made so that when the rod temperatures are increasing not all of the decay heat generated below the swollen liquid level is put into the fluid. Hand calculations have been done to verify that the timing of the uncovering of the core is too short for the old ORNL MARCH version (2200 min, Fig. 6) and that the timing of the uncovering of core as calculated by the new ORNL MARCH version is correct (2255 min, Fig. 5).

One should be aware that in a non-cycling pressure process involving a two phase system, the aforementioned deficiency in MARCH^{5,6} is a non issue. However in realistic modeling of the BWR SRV induced pressure changes, this deficiency is most prominent. SRVs often undergo hundreds of cycles during long accident transients and the error produced due to the MARCH^{5,6} deficiency accumulates with each SRV cycle.

The liquid mass inventory is shown in Figs. 7 and 8 for the old and new versions respectively. As mentioned earlier, we chose to match the CLL between the two versions at the beginning of the calculation. Because of the different vessel geometries modeled below the CLL, and because of the differing densities of liquid residing in the vessel below the CLL, the liquid mass residing in the vessel for the old version is less than that of the new version. The increased boiloff so readily apparent in the CLL comparisons (Figs. 5 and 6) is also evident in the rate of change of mass between the two versions.

The calculated swollen mixture levels are shown in Figs. 9 and 10 for the old and new versions, respectively. The flat level peaks seen early in the calculation in the old version, Fig. 9, are an artifact of the way MARCH⁵ calculated swollen level. For swollen levels greater than the top of the heated length, MARCH⁵ added the collapsed liquid level to the product of the average void fraction and the height of the core. For the new version, a different artificiality is employed when the swollen level is above the top of the core. In this case, the swollen level is limited to the level of the top of the steam separators, i.e. 607.5 inches (15.4 m) above vessel zero. The effects of SRV actuations are clearly evident in both cases as the two phase region swells appreciably [~ 100 inches (2.54 m) in some instances] due to the depressurization accompanying a SRV discharge. Once again, the more rapid boiloff of the old version is apparent.

Figures 11 and 12 show calculated gas temperatures exiting the top of the core for the old and new versions respectively. Both Figures show the gas temperature as being at the saturation temperature for 1090 psia (7.515×10^6 Pa), i.e. about 555°F (290.6°C), and then becoming superheated as the swollen mixture level drops below the top of the core. Because the level drops faster in the old version than the new, the superheating of the gas temperature occurs sooner in the old version. Also of interest are the downward spikes evident in the new version. These spikes represent less superheating of the core exit gases as the swollen level rises due to SRV actuations. Also apparent in the old version are periods of zero steam flow where the code artificially sets the core exit temperature to the saturation temperature. Note too, that there are no periods of zero steam flow in the core for the new version.

Figures 13 and 14 show calculated fuel temperature for a fuel node located in the upper end of the core. Because the old version boils off faster than the new version, the rod temperature in the old version becomes elevated about 40 minutes earlier than in the new version. The effects of SRV cycling are evident in both figures. Calculated fuel temperature is $\sim 1000^\circ\text{F}$ ($\sim 537^\circ\text{C}$) cooler in the new version than in the old version at the end of the calculation.

Figures 15 and 16 show the cumulative energy produced as a result of the fuel rod cladding zirconium/steam reaction for the old and new

versions respectively. Because the old run produced higher rod temperatures than the new run, the zirconium/steam reaction was more vigorous in the old run than in the new.

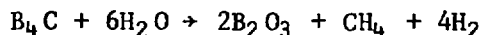
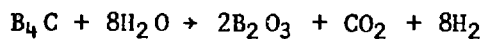
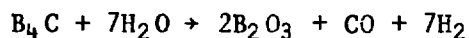
Figure 17 shows the total steaming rate as a function of time as calculated by ORNL's new version of MARCH. A solid curve is apparent which is representative of the steaming rate due to boiling with stair step decreases near the end of the calculation. These decreases correspond to the axial levels of the core becoming uncovered. The spikes above the curve correspond to the steaming produced as a result of the flashing accompanying the depressurization resulting from SRV discharges. The spikes below the solid curve denote diminished boiling due to the flow of cooler liquid from regions outside the core to those inside the core.

Ongoing and Future SASA Work

Additional model development is underway or is planned for the future. Areas which are being addressed include the following (1) thermal stratification modeling for the BWR pressure suppression pool, (2) incorporation of B₄C/steam reaction models, (3) development of a phenomenological model of corium mass transport from the intact rod geometry through rod slump, vessel failure, and relocation on the drywell floor, and (4) incorporation of an advanced corium/concrete interaction model. Each of these areas of work will now be addressed.

A model for thermal mixing in a BWR MARK I pressure suppression pool has been developed.⁷ ORNL believes the additional detail of the space/time temperature distributions provided by Dr. Cook's algorithm is necessary in order to realistically assess total pool evaporation rate. It is a comprehensive analytical tool which is also capable of calculating the phenomenon whereby SRV discharge is not condensed but bypasses the pool and directly enters the wet well atmosphere.

Next, ORNL SASA is in the process of including models which address the thermochemical effects of the various boron carbide/steam reactions. The various reactions are:



The above chemistry was derived by Dr. Ed Beahm.⁸ The reactions are exothermic and large quantities of H₂ are produced as well as CO, CO₂, and CH₄, of which H₂, CO, and CH₄ are combustible. Also the borates produced in these various reactions can further react with compounds containing fission products (such as CsI) thus altering the final chemical form of fission products.

The next area to be addressed in ORNL SASA efforts is in corium mass transport. At present there is no one code which mechanistically tracks corium transport from the "loss of geometry" stage all the way through to the point when corium contacts the drywell floor. Early MARCH models assumed core slumping occurred at a user input fraction of the total core melt. This is not realistic for a BWR core because each group of four fuel assemblies is independently supported from below. The bottom core plate provides no vertical support, only lateral support. Therefore core material relocation must be done on a more localized basis. Models for such localized material relocation are under development by subcontracted effort at RPI.⁹ Coupled with these models are the development of models which realistically evaluate corium attack on the lower vessel head.

Because realistic core relocation models will not collapse the core uniformly, the release of volatile fission products will be distributed in time. The importance of the timing of each release relative to lower head failure and containment failure is obvious. Suppression pool scrubbing of SRV discharge disappears once the lower head of the vessel fails.

The final phenomenon that ORNL SASA investigators are addressing is the corium/concrete interactions which occur once the corium relocates to the concrete floor of the drywell. The importance of accurately modeling such interactions lies in the effects of the evolved gases entering the drywell atmosphere. Because the primary containment is relatively small, containment response is sensitive to the gases produced as a result of corium/concrete interaction. The evolved gases are very hot and can act to raise both the pressure and temperature of the primary containment, both of which are possible containment failure mechanisms. In addition, if the corium pool spreads wide enough, contact can be made directly with the drywell liner, and failure of the containment may occur.

Therefore for all of the above reasons, it is important to use an advanced code to calculate corium concrete interactions. Such a code exists; it is called CORCON MOD2¹⁰, and the SASA program at Sandia National Laboratory has incorporated it into a prereleased version of MARCH 2.0. The combined code has been named MARCON 2.0B. At the present time ORNL researchers are implementing the models described earlier in this paper into MARCON 2.0B.

Summary

In summary, it is important to realize that BWRs have unique features which must be modeled for best estimate severe accident analysis. ORNL has developed and incorporated into its version of MARCH several improved models. These include (1) channel boxes and control blades, (2) SRV actuations, (3) vessel water level, (4) multi-node analysis of in-vessel water inventory, (5) comprehensive hydrogen and water

properties package, (6) first order correction to the ideal gas law, and (7) separation of fuel and cladding.

Ongoing and future modeling efforts are required. These include (1) detailed modeling for the pressure suppression pool, (2) incorporation of B₄C/steam reaction models, (3) phenomenological model of corium mass transport, and (4) advanced corium/concrete interaction modeling.

REFERENCES

1. D. H. Cook et al., "Station Blackout at Browns Ferry Unit One — Accident Sequence Analysis," NUREG/CR-2182, November 1981.
2. S. R. Greene et al., "SBLOCA Outside Containment at Browns Ferry Unit One — Accident Sequence Analysis," NUREG/CR-2672, November 1982.
3. S. A. Hodge et al., "Loss of DHR Sequences at Browns Ferry Unit One — Accident Sequence Analysis," NUREG/CR-2973, May 1983.
4. L. J. Ott et al., "The Effect of Small-Capacity, High Pressure Injection Systems on TQUV Sequences at Browns Ferry Unit One," NUREG/CR-3179, September 1983.
5. Roger O. Wooten and Halil I. Arci, "MARCH (Meltdown Accident Response Characteristics) Code Description and User's Manual," NUREG/CR-1711, October 1980.
6. Roger O. Wooten et al., "MARCH 2 (Meltdown Accident Response Characteristics) Code Description and User's Manual," NUREG/CR-3988, August 1984.
7. D. H. Cook, "Pressure Suppression Pool Thermal Mixing," NUREG/CR-3471, October 1984.
8. E. C. Beahm, "Chemical Factors Affecting Fission Product Transport in BWR Severe Accidents," Twelfth Water Reactor Safety Research Information Meeting, October 1984.
9. B. R. Koh et al., "The Modeling of BWR Core Meltdown Accidents — For Application in the MELRPI.MOD2 Computer Code," NUREG/CR-3889, ORNL/Sub/81-9089/2, December 1984.
10. R. H. Cole et al., "CORCON-MOD2: A Computer Program for Analysis of Molten-Core Concrete Interactions," NUREG/CR-SAND84-1246, to be published.

Table 1. Identification of model differences between current and old ORNL versions of MARCH. "Yes" indicates the model is included, while "No" means it is not

Model designator	ORNL-current	ORNL-old
Separated fuel & cladding	Yes	No
Axial conduction	Yes	No
Improved heat transfer correlations for uncovered region of core	Yes	No
Mechanistic rod models in water covered region	Yes	No
BWR canister and control blades	Yes	Yes
BWR SRV models	Yes	Yes ^a
New pressure calculation algorithm	Yes	No
BWR level routine	Yes	No
Multi-node analysis of invessel water inventory	Yes	No
New boiling and flashing algorithm	Yes	No
New Zr/steam reaction model	Yes	No
"Melt" models for canisters and control blades	Yes	Yes
New H ₂ /H ₂ O physical properties package	Yes	Yes ^b

^aImproved over original MARCH,⁵ but still not as mechanistic as in the current ORNL version.

^bOld version was improved over original MARCH,⁵ but still not as comprehensive as in the current ORNL version.

THE BWR CORE CONTAINS MANY CONTROL BLADES; EACH FUEL ASSEMBLY IS SURROUNDED BY A CHANNEL BOX

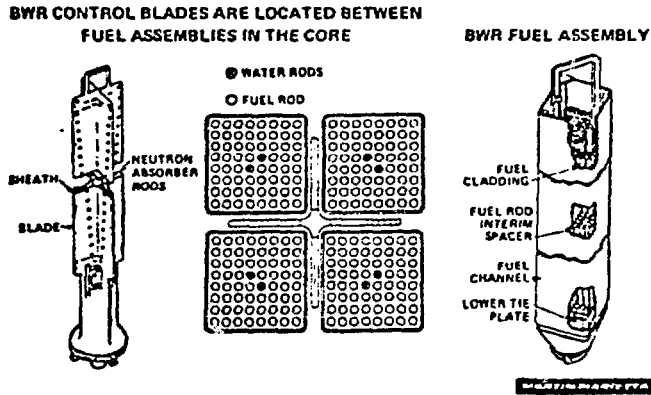
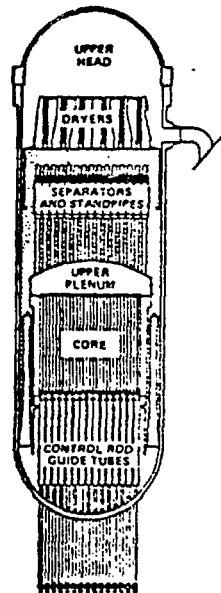


Fig. 1. Schematic of BWR control blade and fuel assemblies.

ACCURATE REACTOR VESSEL WATER LEVEL DETERMINATION IS IMPORTANT TO BWR SEVERE ACCIDENT ANALYSES



LARGE LIQUID INVENTORIES IN LOWER PORTION OF REACTOR VESSEL MUST BE MODELED SEPARATELY

Fig. 2. Schematic of BWR invessel structures.

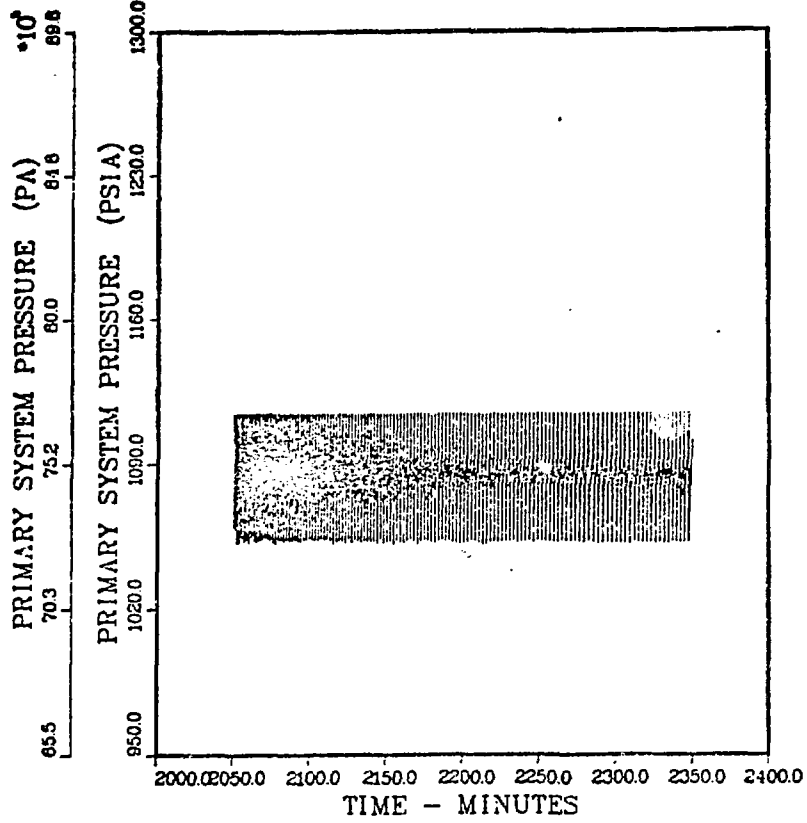


Fig. 3. Pressure results from new ORNL MARCH version.

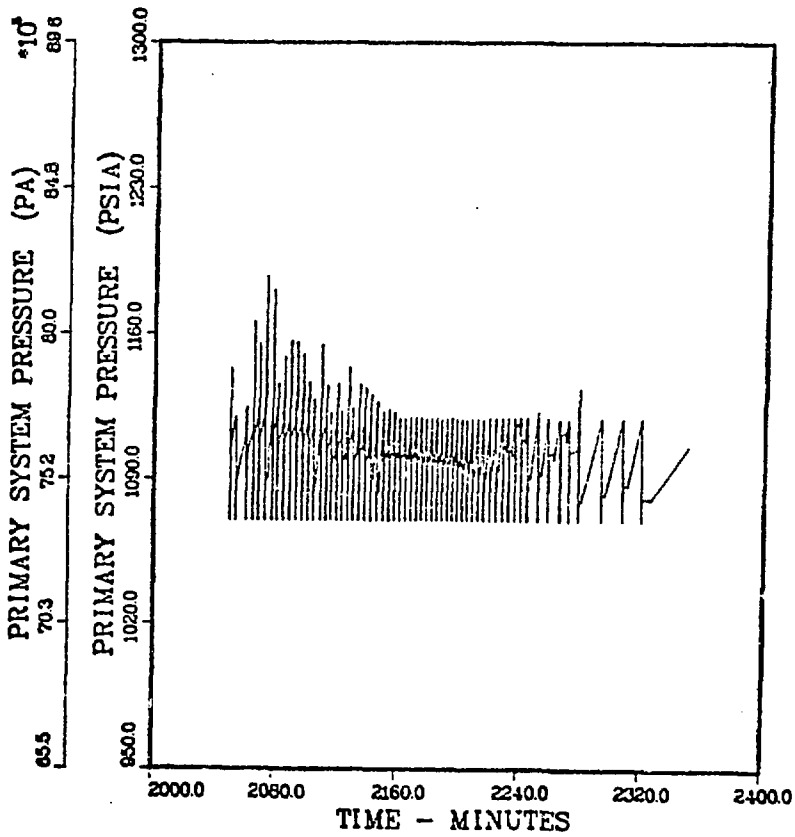


Fig. 4. Pressure results from old ORNL MARCH version.

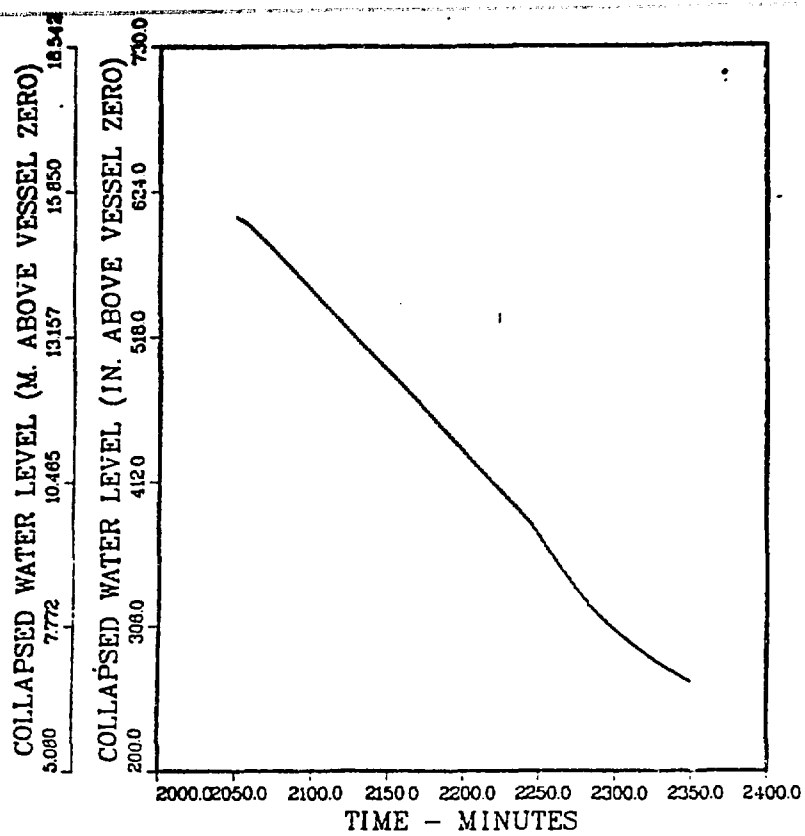


Fig. 5. Collapsed liquid level results from new ORNL MARCH version.

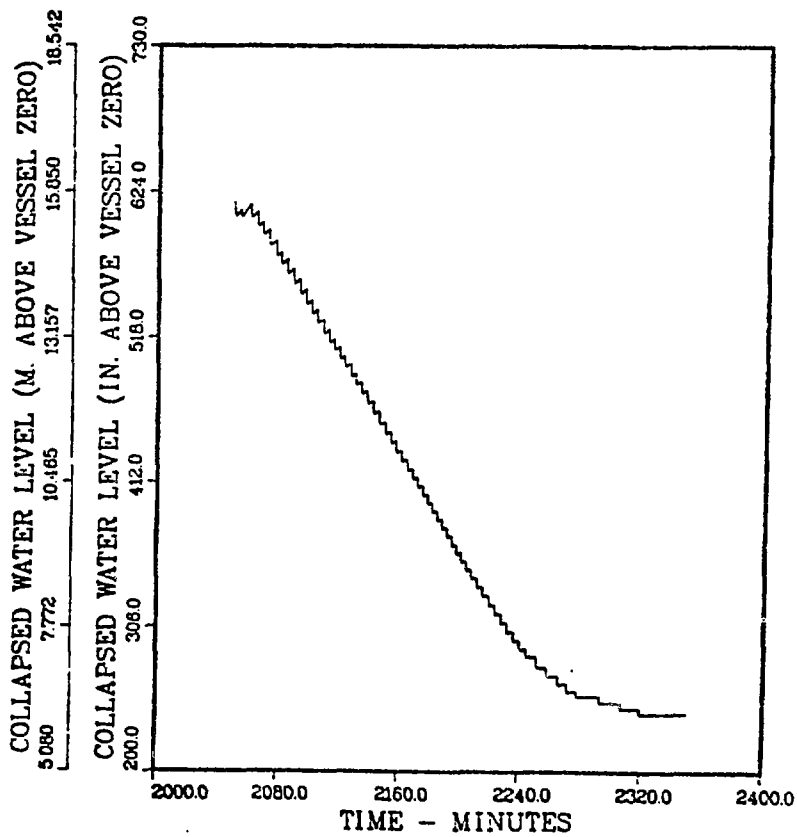


Fig. 6. Collapsed liquid level results from old ORNL MARCH version.

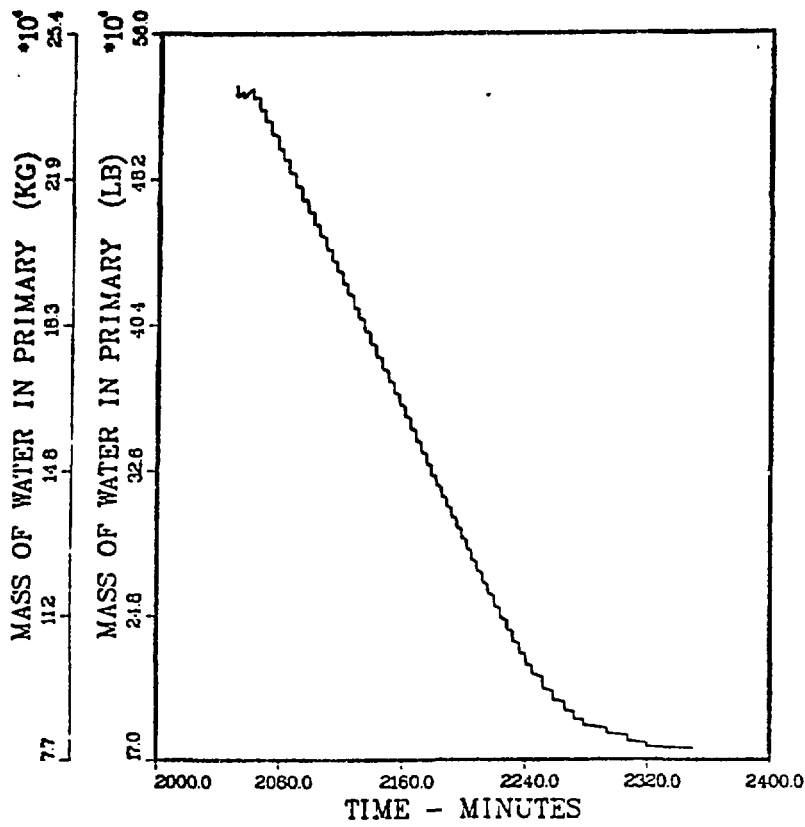


Fig. 7. Liquid mass inventory results from old ORNL MARCH version.

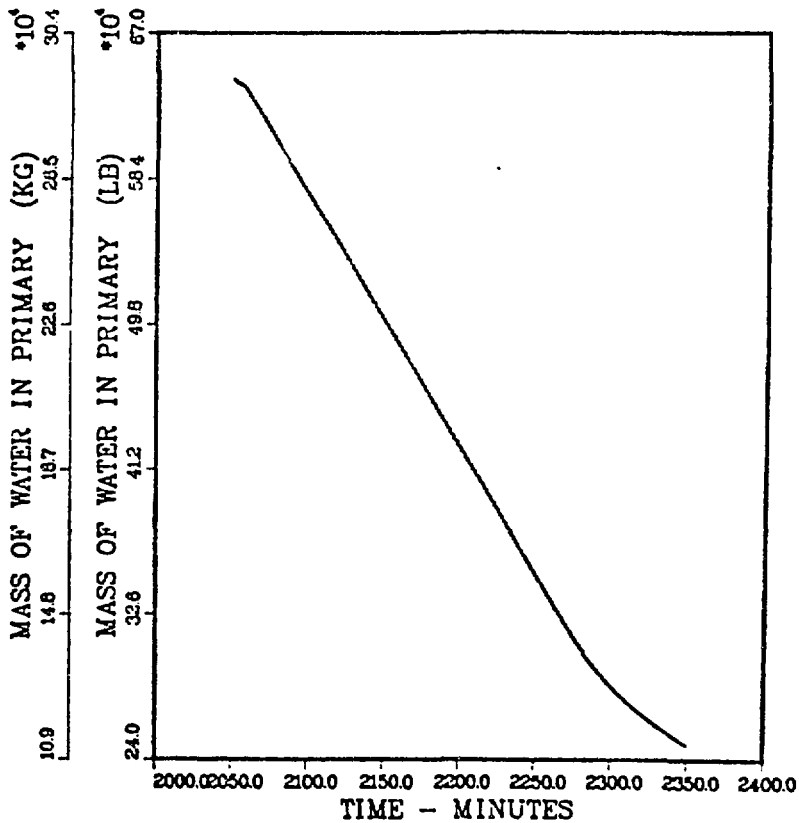


Fig. 8. Liquid mass inventory results from new ORNL MARCH version.

Fig. 10. Swollen mixture level results from new ORNL version of MARCH.

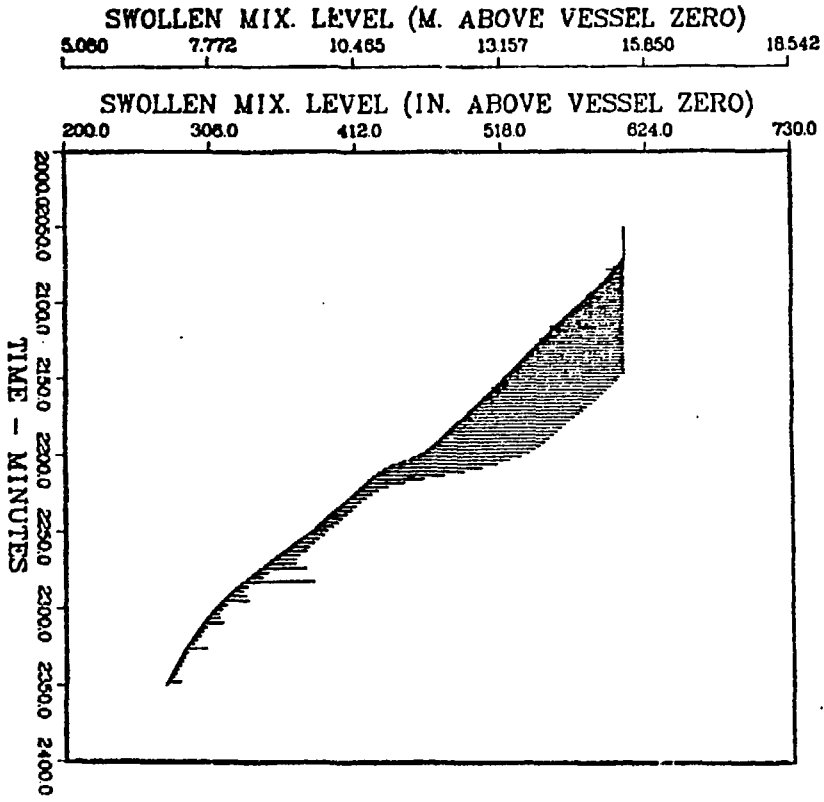
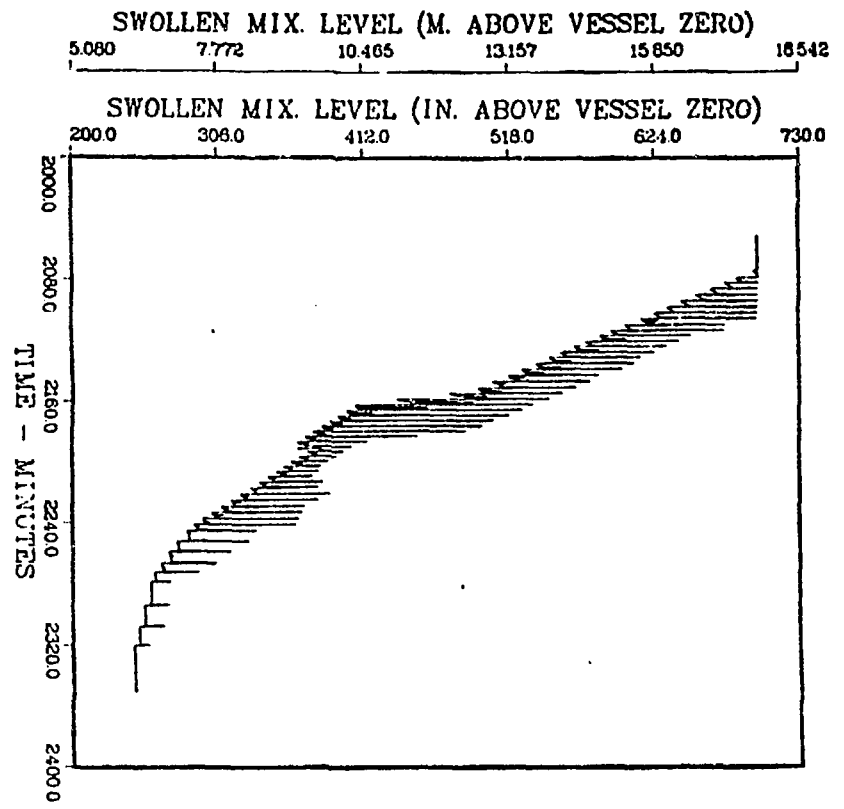


Fig. 9. Swollen mixture level results from old ORNL version of MARCH.



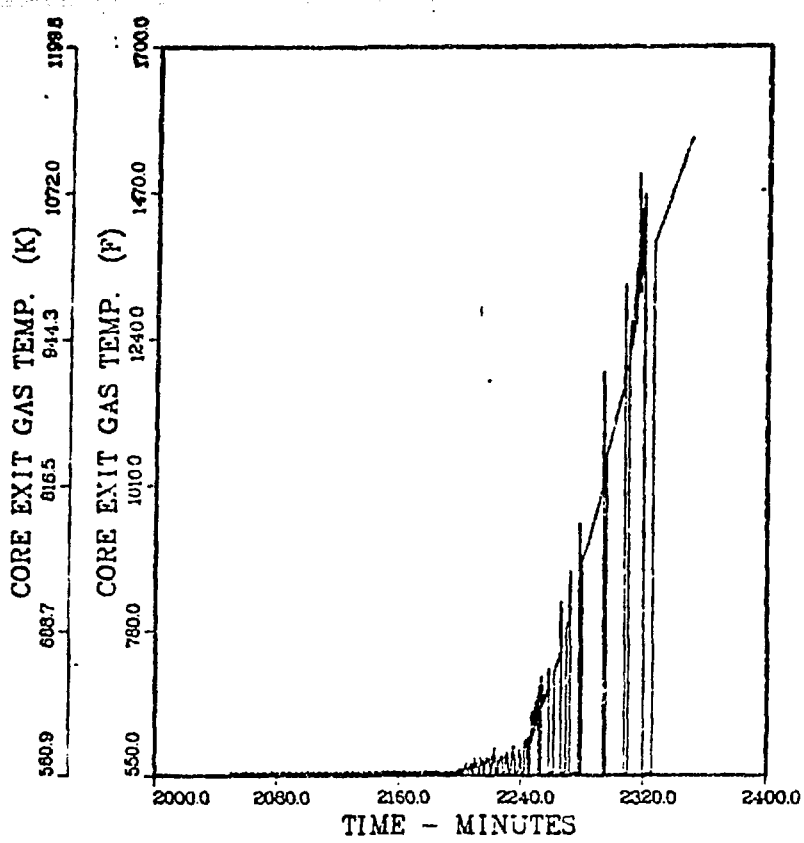


Fig. 11. Core exit gas temperature, from old ORNL version of MARCH.

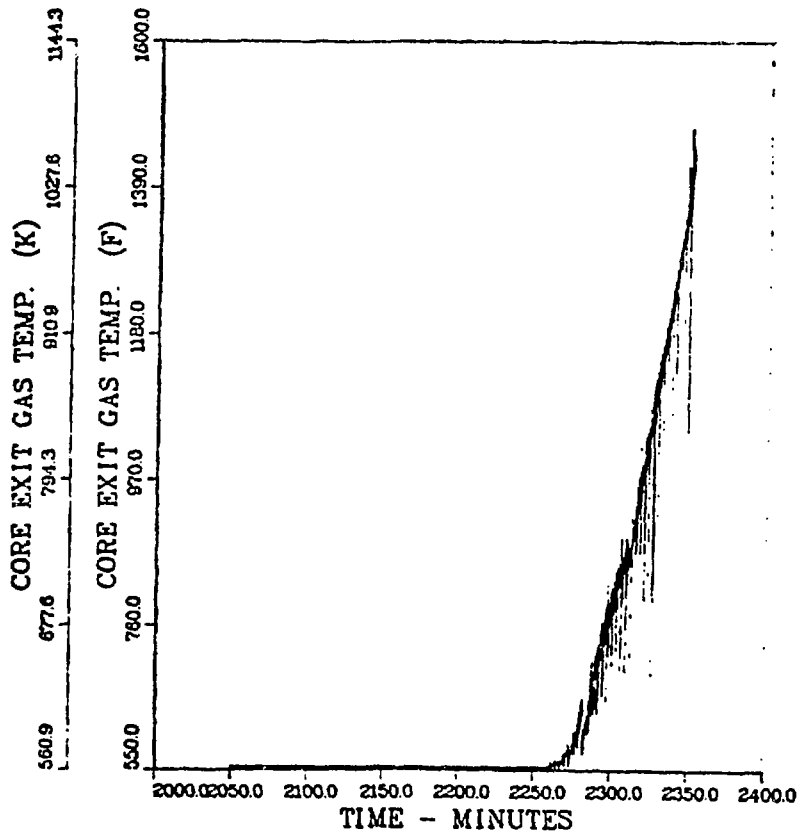


Fig. 12. Core exit gas temperature, from new ORNL version of MARCH.

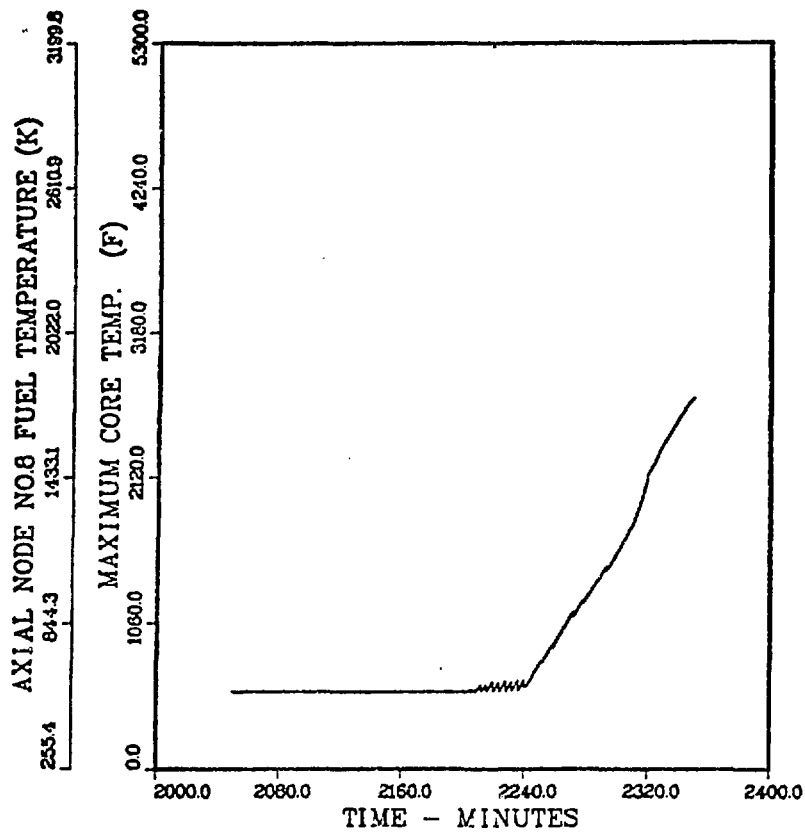


Fig. 13. Upper fuel node temperature from old ORNL version of MARCH.

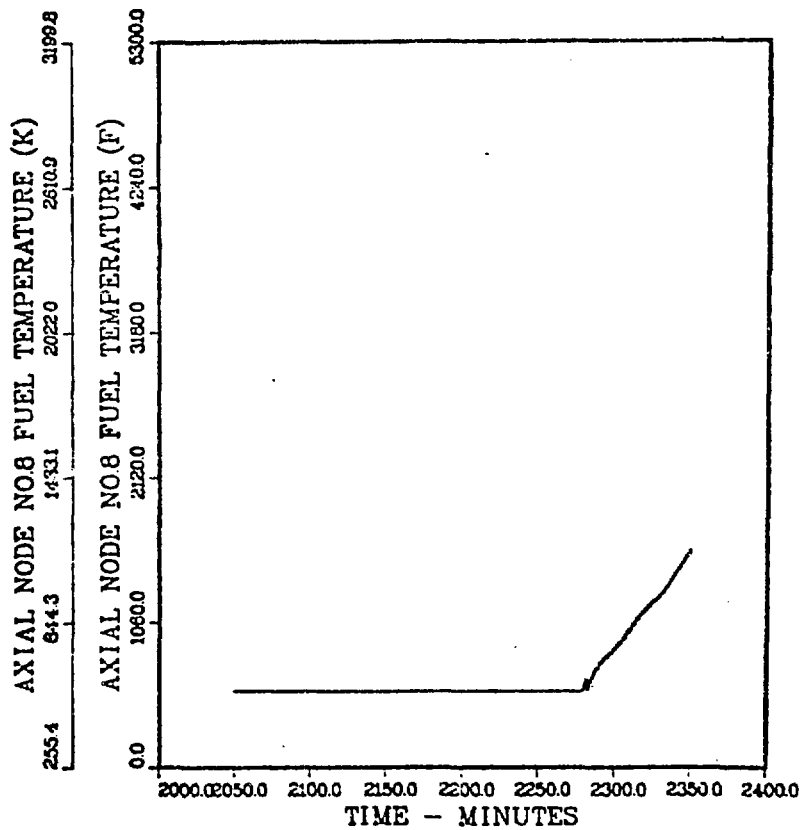


Fig. 14. Upper fuel node temperature from new ORNL version of MARCH.

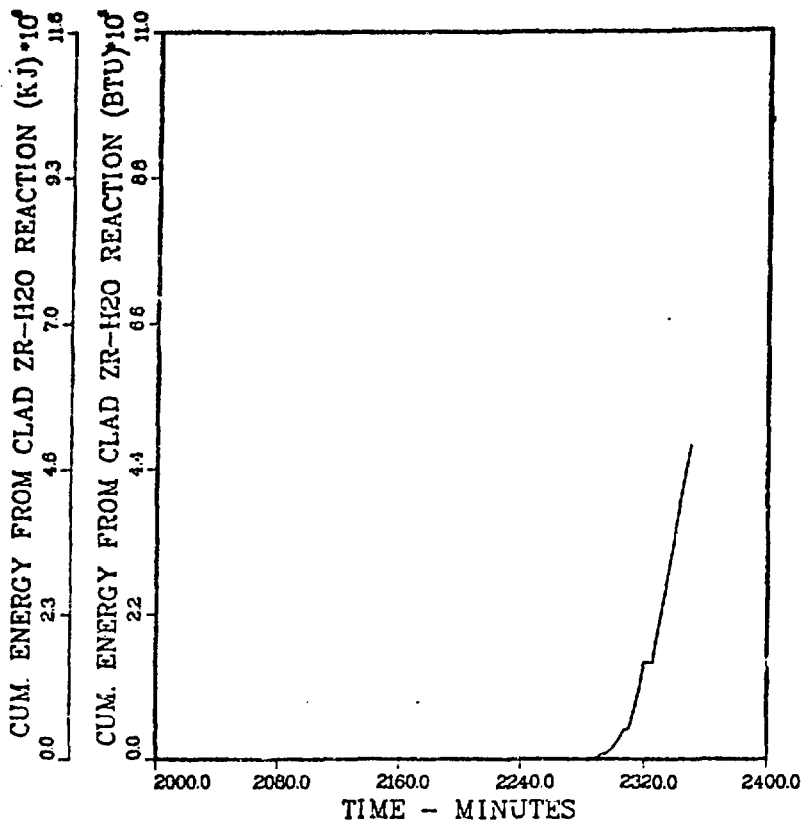


Fig. 15. Cumulative energy from fuel cladding zirconium/steam reaction from old ORNL version of MARCH.

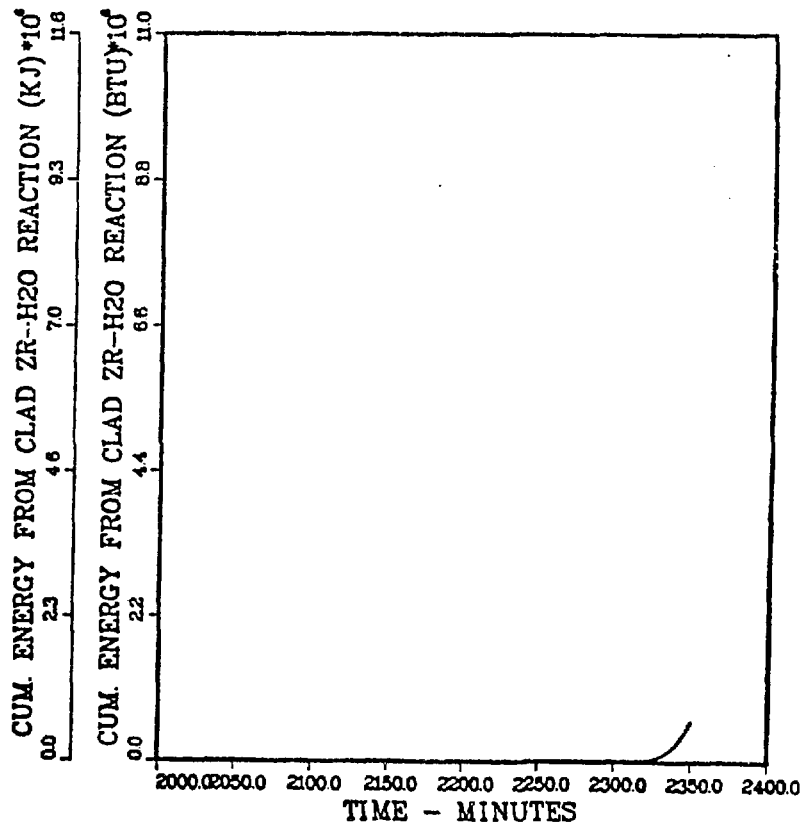


Fig. 16. Cumulative energy from fuel cladding zirconium/steam reaction from new ORNL version of MARCH.

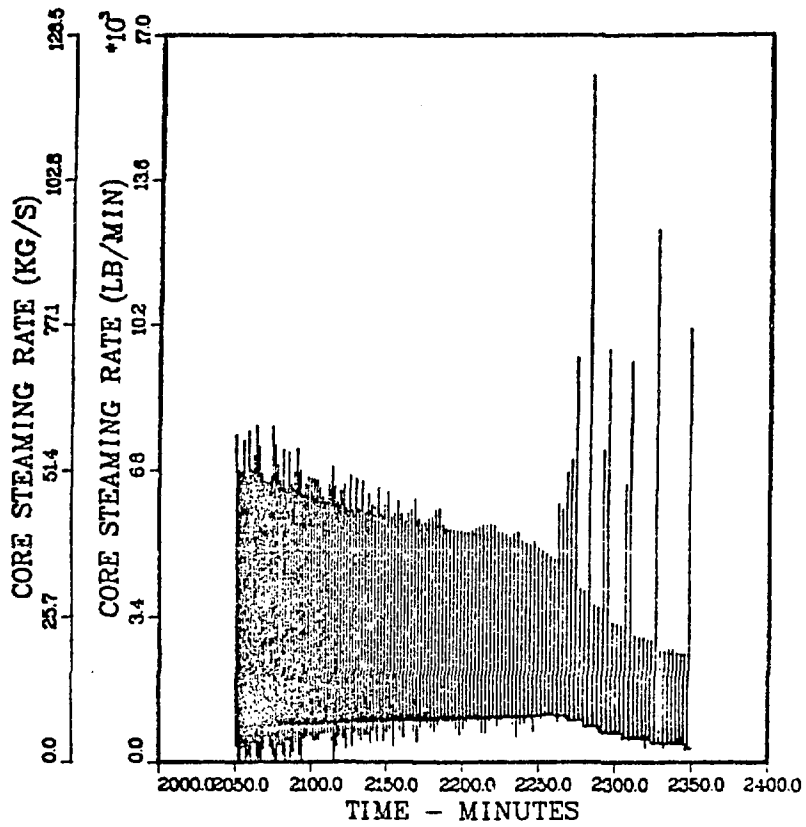


Fig. 17. Total steaming rate from new ORNL version of MARCH.